Structure and dynamics in solution of the stop codon decoding N-terminal domain of the human polypeptide chain release factor eRF1

Vladimir I. Polshakov[1], Boris D. Eliseev[2], Berry Birdsall[3], and Ludmila Yu. Frolova[2]

[1] Center for Magnetic Tomography and Spectroscopy, Faculty of Fundamental Medicine, M.V.Lomonosov Moscow State University, Moscow 119991, Russia;

[2] Engelhardt Institute of Molecular Biology, Russian Academy of Sciences, 119991 Moscow, Russia;

[3] Division of Molecular Structure, National Institute for Medical Research, The Ridgeway, Mill Hill, London NW7 1AA, U.K.

Supporting Material

NMR dynamics analysis

NMR experiments for the measurement of ^{15}N longitudinal relaxation rates R_1, transverse relaxation rates R_2 and $^{15}N\{^1H\}$ heteronuclear NOE values, were collected on a ~1 mM ^{15}N-labelled N-eRF1 sample at 298 K with a Varian INOVA 600 MHz NMR spectrometer using pulse sequences [1] modified to compensate for cross-correlation effects [2]. The delays for the R_1 relaxation rate experiments were 8.63, 96.96, 193.32, 297.71, 394.07, 498.46, 594.82, 795.57, 996.32, 2000.07, 2995.79 ms; and for the R_2 relaxation rate experiments were 8.65, 17.3, 25.95, 34.6, 43.25, 51.9, 69.2, 86.5, 103.8, 129.75 and 147.05 ms. The irradiation time for ^1H in the ^1H-^{15}N heteronuclear NOE experiments was 4.0 s.

Spectra were processed using NMRPipe software [3]. The nonlinear fitting of the integrated peak volumes in the pseudo 3D spectra of the relaxation experiments and the calculation of standard deviations were accomplished using the nlinLS procedure. Obtained relative peak intensities were used in the calculations of R_1 and R_2 values using written in-house RelaxFit program [4]. The standard deviations

of the $^{15}N\{^{1}H\}$ NOE values were calculated using the RMS noise of the background regions [5] and were further checked and corrected using two independently collected experimental data sets.

The analysis of the R_1, R_2 and $^{1}H,^{15}N$-NOE values was carried out using a model-free formalism using the RelaxFit program. The overall correlation time was calculated from the R_2/R_1 ratios [1]. The calculations yield an average overall correlation time value of 11.04 ± 0.16 ns at 298K. The overall correlation time was treated as a fixed parameter in subsequent analysis of the relaxation data.

Experimental values of the relaxation parameters were interpreted using the model-free formalism [6] with extensions to include slower internal motions [7] and chemical exchange contributions R_{ex} to the transverse relaxation rates [8] under the assumptions of both isotropic and axially symmetric anisotropic rotational diffusion. Several motional models that included combination of optimized internal motion parameters S^2 (order parameter), τ_e (effective correlation time of internal motion) and R_{ex} (chemical exchange contribution to the transverse relaxation rate) were used. All calculations were carried out using the program RelaxFit written-in-house [4].

The magnitude and rhombicity of an axially symmetric rotational diffusion tensor were determined in a similar manner to that described previously for the M-domain of human eRF1 [9] using a graphical comparison of the experimentally measured parameters against the simulated datasets (Fig. S6). The data shown by the red dots were simulated at 600 MHz proton resonance frequency using Clore's extension of the Lipari and Szabo formalism [7] and axially symmetric diffusion models with the following parameters randomly generated (1000 data sets) using a Gaussian distribution: average rotational correlation time τ_c 11.04 ns; ratio of the principal axis of the axially symmetric diffusion tensor ($D_{\parallel}/D_{\perp}$) 1.6 ± 0.1; order parameter S^2_{slow} between 0.3 and 1.0; correlation time of fast motion between 0 and 50 ps; correlation time of slow motion τ_{slow} 1.05 ± 0.05 ns; order parameter of fast motions S^2_{fast} 0.9 ± 0.1. The slope and the distribution of the simulated data are very sensitive to the above parameters. Therefore the good correlation between simulated and experimental data indicates that these parameters can be used to describe the dynamic behavior of the protein backbone. The

parameters τ_{slow} and $D_{\parallel}/D_{\perp}$ were then used in the fitting of residue-specific relaxation data (Fig S5). The uncertainties in the calculated parameters (S^2, R_{ex} and internal motion correlation times) were obtained using 500 cycles of Monte-Carlo simulations [10].

References

1. Kay LE, Torchia DA, Bax A (1989) Backbone dynamics of proteins as studied by ^{15}N inverse detected heteronuclear NMR spectroscopy: application to staphylococcal nuclease. Biochemistry **28**:8972-8979.

2. Boyd J, Hommel U, Campbell ID (1990) Influence of cross-correlation between dipolar and anisotropic chemical-shift relaxation mechanisms upon longitudinal relaxation rates of ^{15}N in macromolecules. Chem Phys Lett **175**:477-482.

3. Delaglio F, Grzesiek S, Vuister GW, Zhu G, Pfeifer J, Bax A (1995) NMRPipe: a multidimensional spectral processing system based on UNIX pipes. J Biomol NMR **6**:277-293.

4. Polshakov VI, Birdsall B, Frenkiel TA, Gargaro AR, Feeney J (1999) Structure and dynamics in solution of the complex of *Lactobacillus casei* dihydrofolate reductase with the new lipophilic antifolate drug trimetrexate. Protein Sci **8**:467-481.

5. Farrow NA, Muhandiram R, Singer AU, Pascal SM, Kay CM, Gish G, Shoelson SE, Pawson T, Forman-Kay JD, Kay LE (1994) Backbone dynamics of a free and phosphopeptide-complexed Src homology 2 domain studied by ^{15}N NMR relaxation. Biochemistry **33**:5984-6003.

6. Lipari G, Szabo A (1982) Model-Free Approach To The Interpretation Of Nuclear Magnetic-Resonance Relaxation In Macromolecules .2. Analysis Of Experimental Results. J Am Chem Soc **104**:4559-4570.

7. Clore GM, Szabo A, Bax A, Kay LE, Driscoll PC, Gronenborn AM (1990) Deviations from the simple 2-parameter model-free approach to the interpretation of ^{15}N nuclear magnetic relaxation of proteins. J Am Chem Soc **112**:4989-4991.

8. Clore GM, Driscoll PC, Wingfield PT, Gronenborn AM (1990) Analysis of the backbone dynamics of interleukin-1 beta using two-dimensional inverse detected heteronuclear ^{15}N-^{1}H NMR spectroscopy. Biochemistry **29**:7387-7401.

9. Ivanova EV, Kolosov PM, Birdsall B, Kelly G, Pastore A, Kisselev LL, Polshakov VI (2007) Eukaryotic class 1 translation termination factor eRF1 - the NMR structure and dynamics of the middle domain involved in triggering ribosome-dependent peptidyl-tRNA hydrolysis. FEBS J **274**:4223-4237.

10. Tillett ML, Blackledge MJ, Derrick JP, Lian LY, Norwood TJ (2000) Overall rotational diffusion and internal mobility in domain II of protein G from Streptococcus determined from N-15 relaxation data. Protein Sci. **9**:1210-1216.

Figure S1. $^{1}H,^{15}N$-HSQC spectrum of the N domain of human eRF1 recorded at 298K. The signals of the minor protein conformer are marked in red.

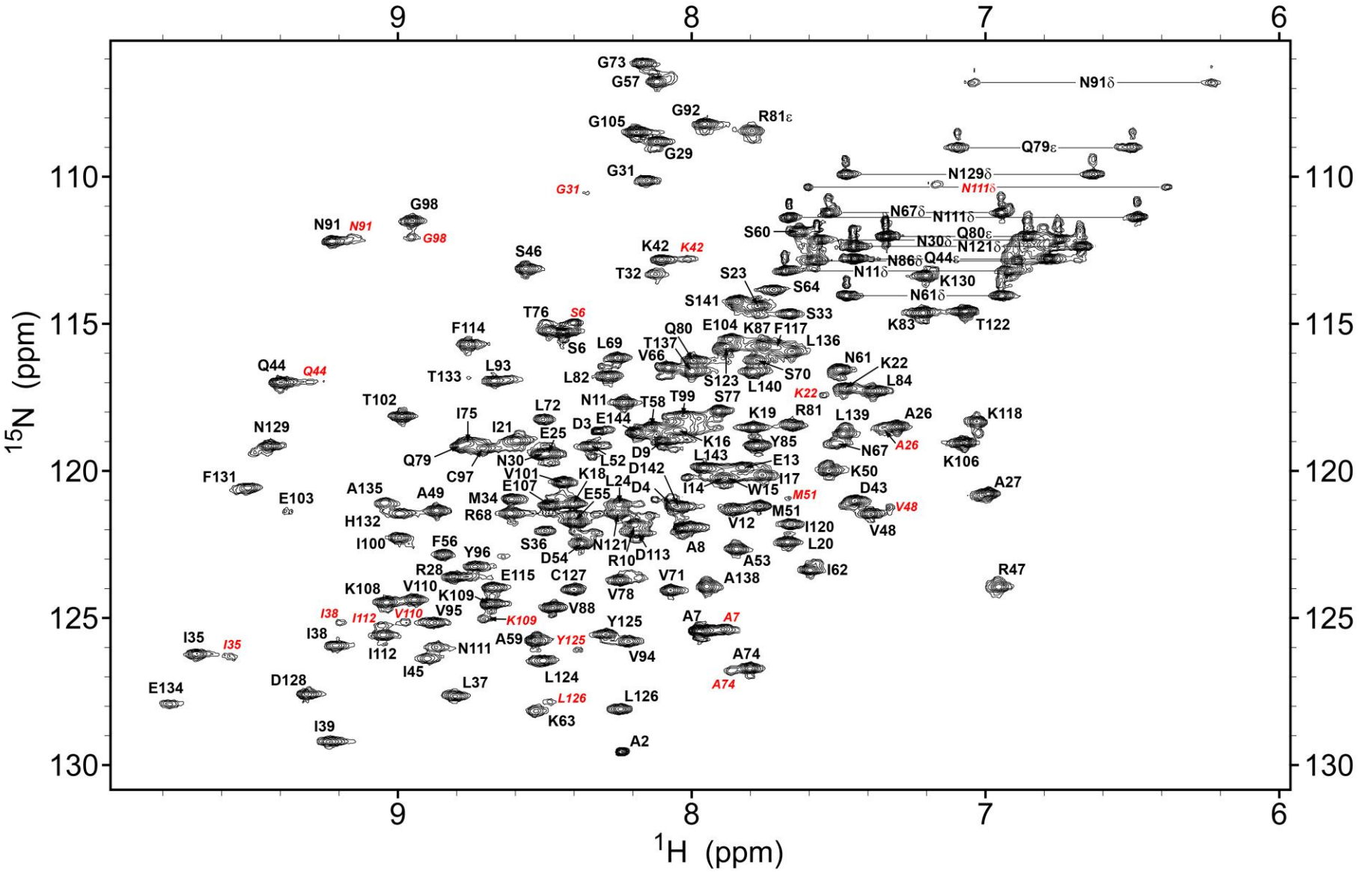

Figure S2. NOE histogram giving the number of long-range (red), medium-range (yellow), sequential (grey) and intra-residue (black) NOEs for each protein residue in the N domain of human eRF1.

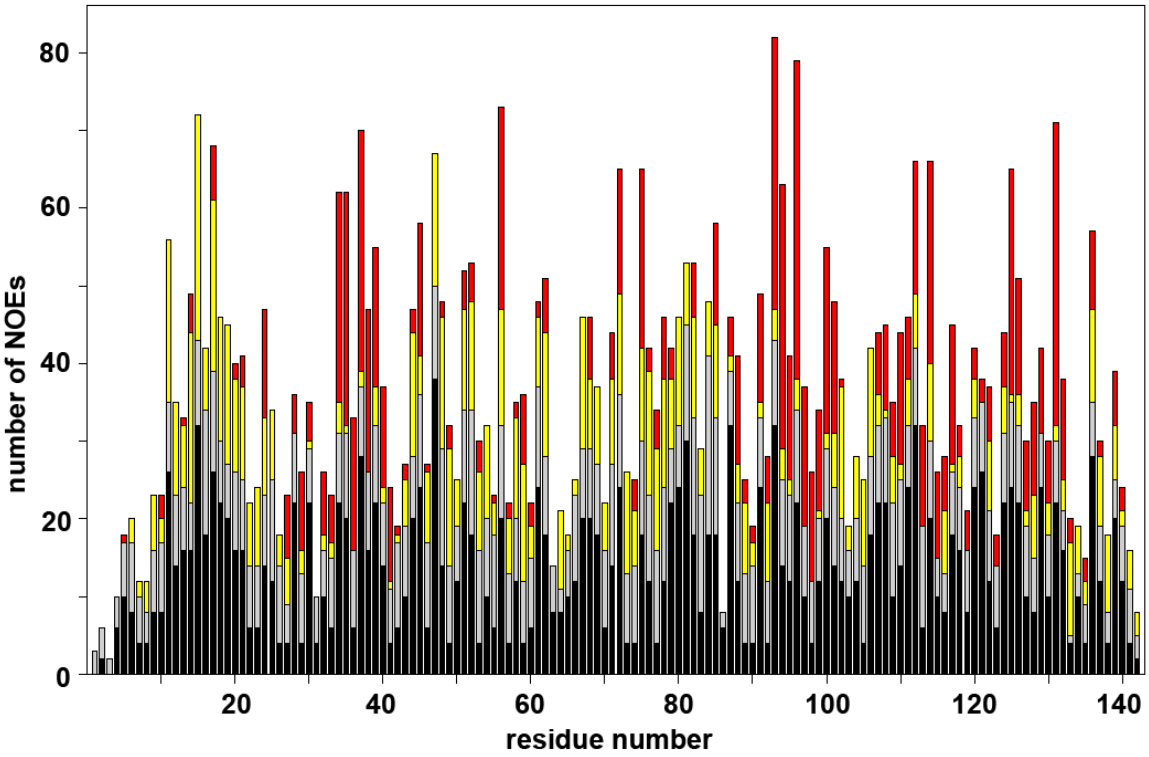

Figure S3. The Ramachandran plot for the final 20 structures of the N domain of human eRF1. No residues fall in disallowed regions, 93.3% of residues fall in the most favourable regions.

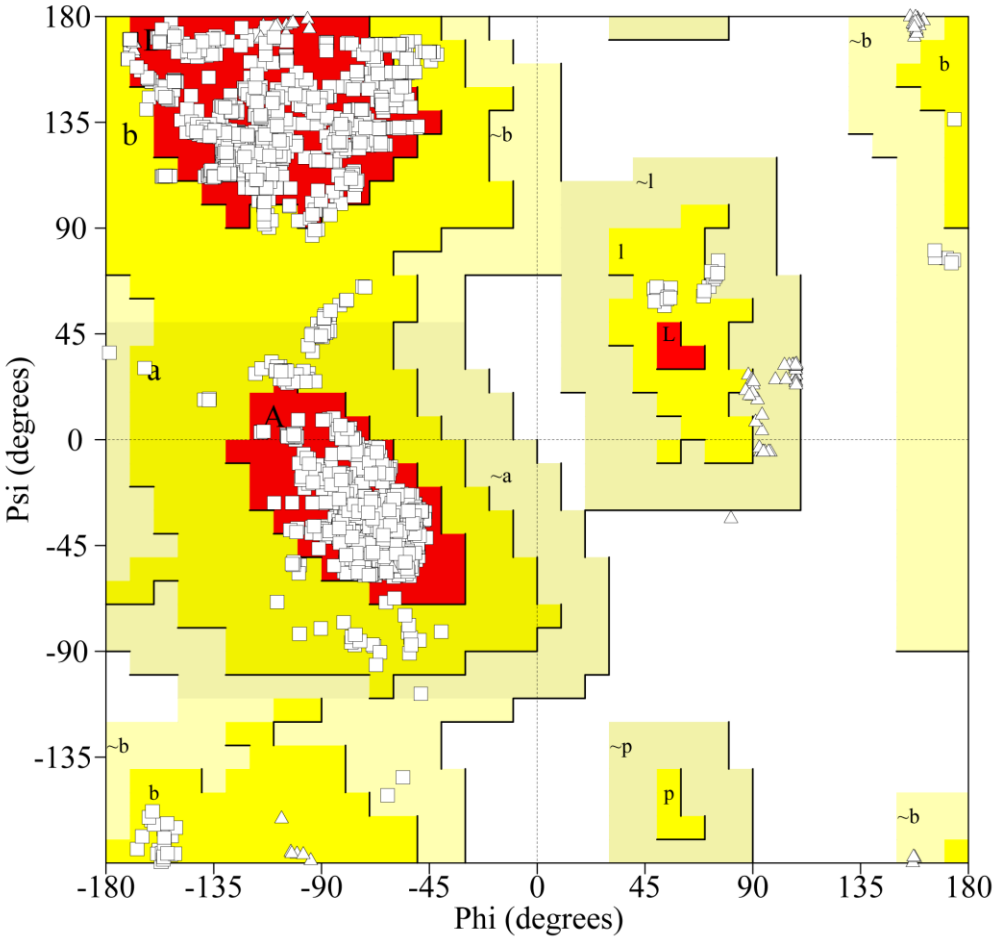

Figure S4. The relaxation parameters of the amide ^{15}N nuclei of each residue of the N domain of human eRF1, measured at 14 T (600 MHz proton resonance frequency) and 298 K. The values shown are those of the longitudinal relaxation rate, R1 (s^{-1}), transverse relaxation rate, R2 (s^{-1}), heteronuclear $^{15}N,^{1}H$-steady-state NOE values, the order parameter S^2, determined by model-free analysis and chemical exchange R_{ex} contributions to the transverse relaxation rates (s^{-1}).

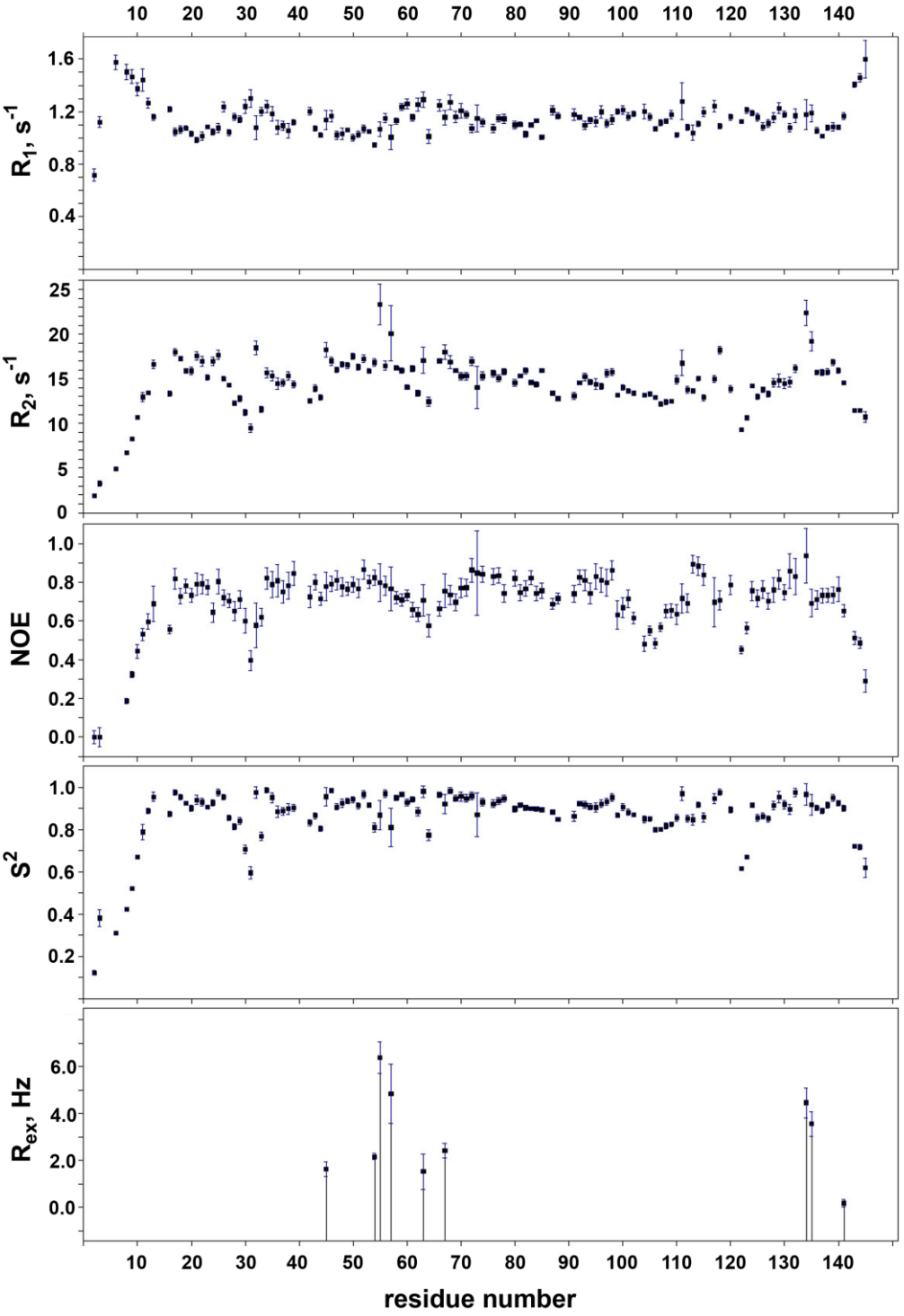

Figure S5. The distribution of the experimental (black squares) and simulated (small red dots) ratios of relaxation rates R_2 / R_1 vs. the heteronuclear $^{15}N,^{1}H$-NOE values. The data were simulated at 600 MHz proton resonance frequency using Clore's extension of the Lipari and Szabo model. The axial symmetry with the ratio $D_{\parallel}/D_{\perp}$ of the principal axis of the tensor was 1.6 ± 0.1; the value of effective overall correlation time $1 / (2D_{\parallel} + 4D_{\perp})$ was 11.04 ns; the values of the order parameter S^2_{slow} were between 0.3 and 1.0; the values of the order parameter S^2_{fast} were between 0.8 and 1.0; the values of the internal motion correlation times τ_{slow} were between 1 and 1.1 ns; and the values of the internal motion correlation times τ_{fast} were between 0 and 50 ps.

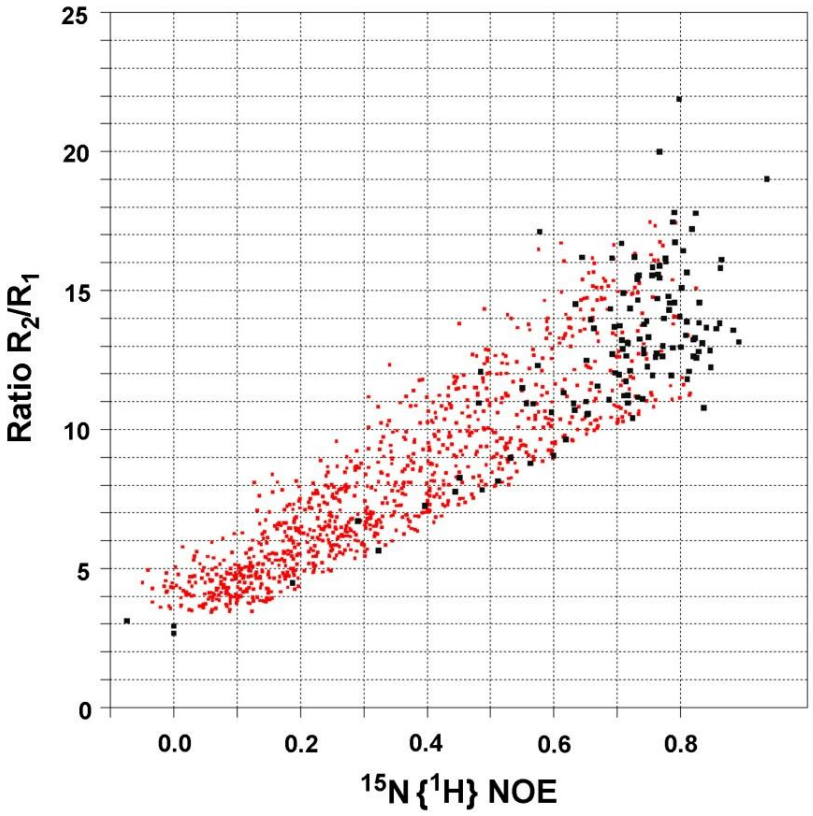

Figure S6. Comparison of the protein backbone flexibility and deviation in its local geometry between solution and crystal structure of the N domain of human eRF1. (A). The order parameter S^2 which reflects the relative amplitude of the protein backbone motions occurring in ps-ns time scale. (B). RMSD values for the heavy atoms of each residue *i* after superposition of the family of 20 NMR structures onto the crystal structure using the set of backbone atoms of four adjacent residues (*i*-2, *i*-1, *i*+1, and *i*+2). Elements of the protein secondary structure are shown on the top of the figure. Regions of the protein with increased backbone flexibility and maximum geometrical differences between the crystal and the solution structures are shaded in yellow.